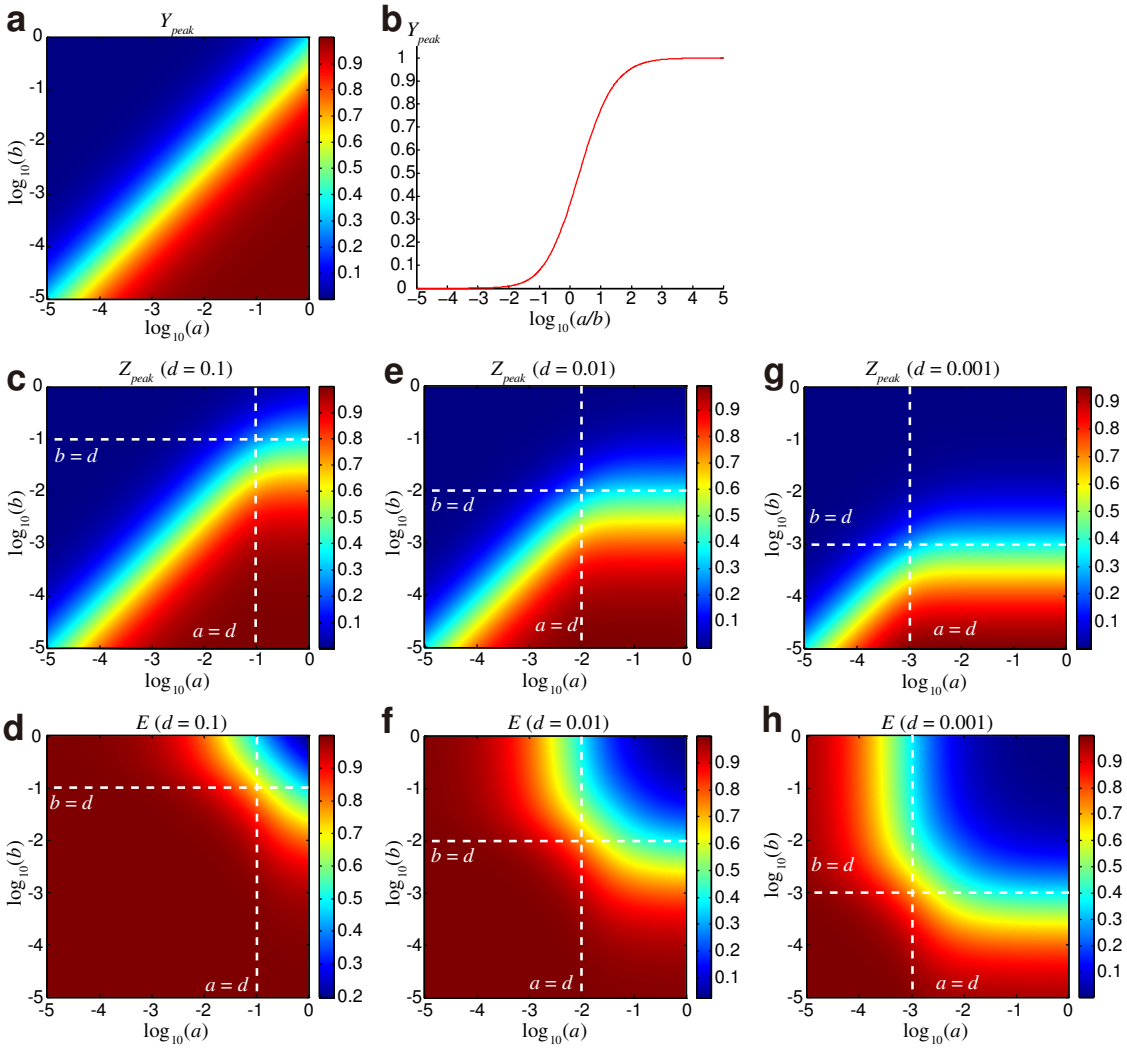

Supplementary Figure S1 | Effect of parameter *d* on Z_{peak} and *E*. (**a**) Y_{peak} against the indicated ranges of *a* and *b*. *c* and *d* did not affect Y_{peak}. The diagonal pattern of the contour line indicates that Y_{peak} was determined by *a*/*b*. (**b**) Y_{peak} for *a*/*b*. (**c**, **e**, and **g**) Z_{peak} against the indicated ranges of *a* and *b* when *d* was set at 0.1, 0.01, and 0.001, respectively. The value of *c* was the same as that of *d*. The white dashed lines indicate when *a* or *b* equals *d*. (**d**, **f**, and **h**) Signal transfer efficiency, *E*, against the indicated ranges of *a* and *b* when *d* was set at 0.1, 0.01, and 0.001, respectively. The value of *c* was the same as that of *d*. *d* affected Z_{peak} and *E*, but did not affect the condition when Z_{peak} became attenuated.

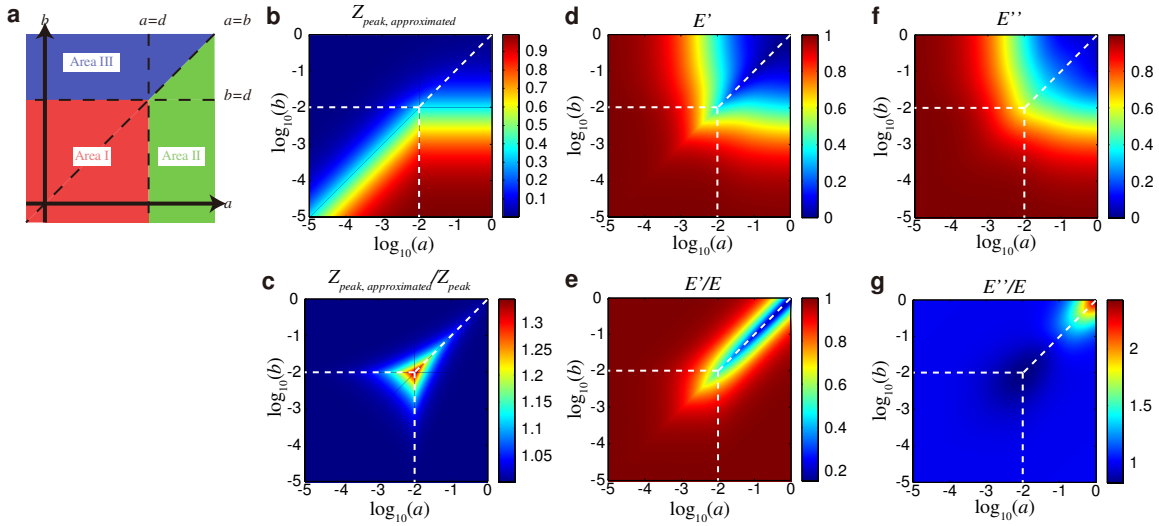

Supplementary Figure S2 | Approximate analytic solution of Z_{peak} and estimation of E. (**a**) The parameter space was divided into three areas. We obtained an approximate analytic solution of Z_{peak} for each area (see Supplementary Note 1). (**b**) Approximate analytical solution of Z_{peak}. The white dashed lines indicate the borders of the areas. (**c**) Ratio of the numerical and the approximate analytic solution of Z_{peak}. The approximate analytical solution of Z_{peak} was very similar to the numerical solution of Z_{peak}. The approximation became inaccurate around the borders of the areas, but the difference between the numerical and analytical values was less than about 35%. (**d**) Estimation of E. The efficiency, E, is not a simple ratio of the peak amplitudes of a single set of upstream and downstream time courses in different scales, but should be scaled by k. We identified a means of estimating E from a single set of upstream and downstream time courses. Based on the approximate analytical solution of Z, the efficiency, E, was expressed in terms of the difference in the peak times, Δt (defined as t_Z - t_Y), and the parameters a and b (see Supplementary Note 1). These values could be obtained from the experimental data of a single set of upstream and downstream time courses. We estimated E from the numerical value of Δt and the parameters a and b. This value was denoted as E' and is shown in colour. (**e**) Ratio of E' to the numerical value of E. E' was very similar to E, but the ratio became extremely low around the borders of areas II and III. (**f**) Estimation of E using an ad hoc substitution. We introduced an ad hoc substitution to estimate E (see Supplementary Note 1) and estimated the value of E based on the new expression. This value was denoted as E'' and is shown in colour. (**g**) Ratio of E'' to the numerical value of E. E'' was very similar to E, and the ratio was closer to 1 than the case for E', indicating an improvement in the estimation. This finding indicates that the signal transfer efficiency E can be estimated from a single set of time courses of Y and Z.

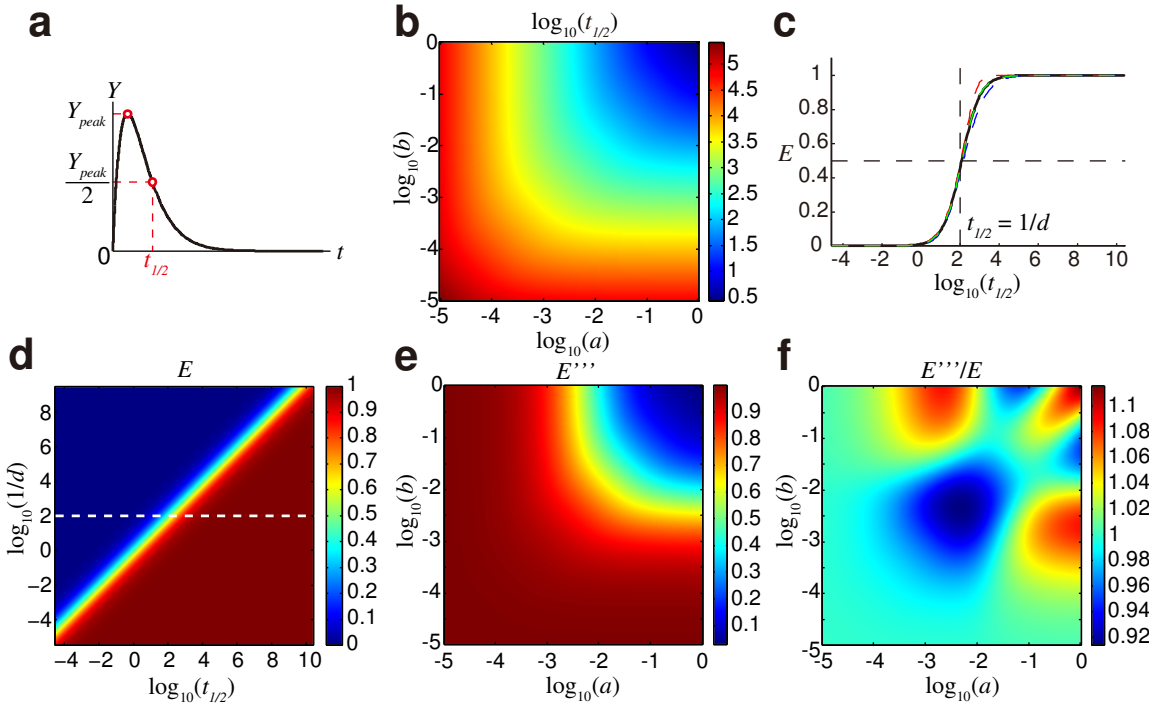

Supplementary Figure S3 | The efficiency *E* can also be estimated from the duration of upstream signal, $t_{1/2}$. (**a**) The duration of upstream signal $t_{1/2}$ is the time at which the value of *Y* has decreased to half of the Y_{peak}. (**b**) $t_{1/2}$ for the indicated ranges of *a* and *b*. The colour indicates $t_{1/2}$ on a logarithmic scale. The concentric pattern of $t_{1/2}$ was similar to that of the efficiency *E* (Fig. 2d) (**c**) Relationship between *E* and $t_{1/2}$. All the data points were plotted in the small area bounded by the red and blue dashed lines. The green dashed line was the midpoint of the red and blue dashed lines. The black solid line shows a sigmoid curve fitted to the green broken line. These lines moved horizontally depending on the value of *d*, and the value of *E* was about 50% when the value of $t_{1/2}$ was the same as that of $1/d$. (**d**) Effect of $t_{1/2}$ and $1/d$ on *E*. The value of $t_{1/2}$ and $1/d$ are shown using a logarithmic scale. The white dashed line corresponds to the black solid line in **c**. The efficiency *E* became smaller when $t_{1/2}$ or *d* became smaller. The diagonal pattern of the contour line indicates that *E* can be estimated by the ratio of $t_{1/2}$ and $1/d$. (**e**) Estimation of the efficiency *E* from $t_{1/2}$. The estimated *E* (*E'''*) was obtained from the numerical value of $t_{1/2}$ and the equation for the fitted sigmoid curve in **c**, $E''' = \dfrac{1}{1+\left(\dfrac{t_{1/2}\cdot d}{1.17}\right)^{-0.932}}$. (**f**) Ratio of *E'''* to the numerical value of *E*. The difference was as much as 10%, indicating that the efficiency *E* can be reasonably estimated using this method when *d* is already known. This method does not require the parameters *a, b,* nor the time course of *Z*.

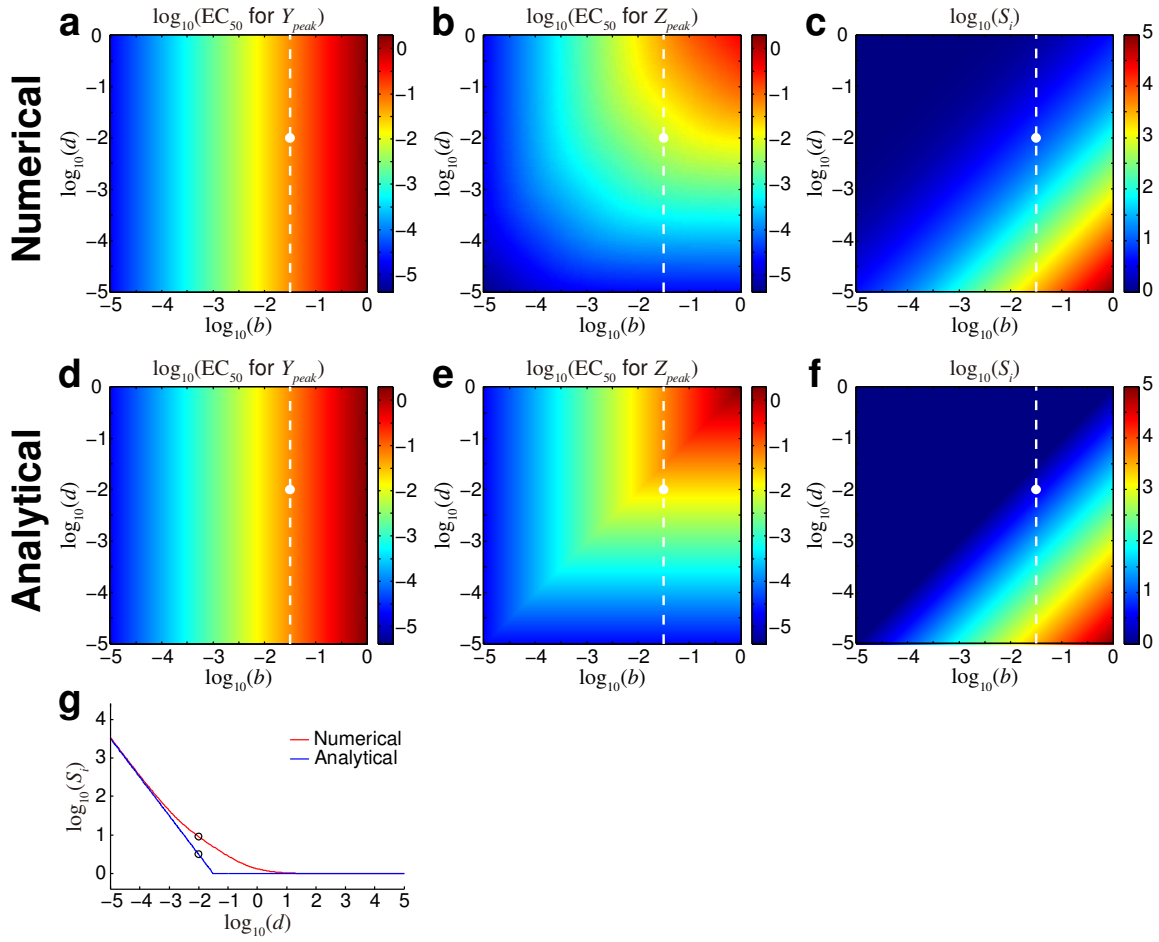

Supplementary Figure S4 | Effect of the parameters on the EC_{50} values and the increase in sensitivity. (**a**-**c**) Numerical results of EC_{50} for Y_{peak}, EC_{50} for Z_{peak}, and S_i, respectively, against the indicated ranges of b and d. The values are shown in colour using a logarithmic scale. The white dot and dashed line indicate the parameters for Fig. 4a-d and e, respectively. The diagonal pattern of the contour line in **c** indicates that S_i is determined by b/d. (**d**-**f**) Analytical solution of EC_{50} for Y_{peak}, approximated analytical solutions of EC_{50} for Z_{peak} and S_i, respectively. Please note that the approximation did not affect the qualitative characteristics of EC_{50} for Z_{peak} and S_i. (**g**) The red and blue line indicates numerical and analytical solutions of S_i , respectively, for the indicated d. The black circles indicate the parameters for Fig. 4a-d.

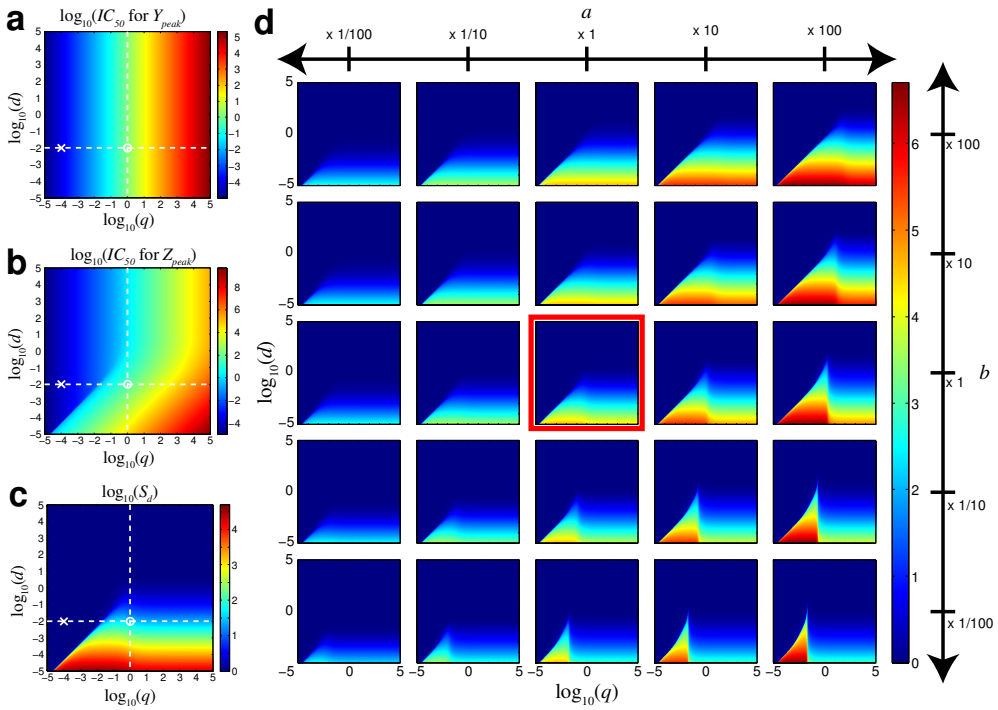

Supplementary Figure S5 | Effect of the parameters on the IC_{50} values and the decrease in sensitivity. (**a** and **b**) IC_{50} values for Y_{peak} and Z_{peak}, respectively, against the indicated ranges of q and d are shown in colour using a logarithmic scale. Both a and b were set at 1. The vertical and horizontal white dashed lines indicate the parameters for Fig. 5f,g, respectively. The white circle and cross indicate the parameters for Fig. 5b-e and Supplementary Fig. S6, respectively. (**c**) S_d for the indicated ranges of q and d is shown in colour using a logarithmic scale. The decrease in sensitivity was suppressed when d was larger than q and when these parameters were relatively small. (**d**) Conditions for the suppression of the decrease in sensitivity for a variety of other parameters. Each panel indicates the S_d against the indicated range of q and d using logarithmic scales for the indicated parameters a and b. The middle panel in the red box is the same as in **c**, although the colour scale is different. The conditions were not affected by the parameters a and b, although S_d depended on these parameters, indicating that the relationship between d and q is an essential and robust index for the suppression of the decrease in sensitivity. When q was relatively small, the dose of the inhibitor induced time courses of Y that were almost proportional with each other (Supplementary Fig. S6). When the time courses of the upstream molecule of the consecutive first-order reaction were proportional with each other, that of the downstream molecule was also proportional with each other. Thus, the proportional relationship was conserved between the upstream and downstream molecules, resulting in the suppression of the decrease in sensitivity. The proportional relationship gradually disappeared with time, and the duration of the proportional relationship became shorter when q became larger. When d became smaller, the peak time of Z became later and the non-proportional part of the time courses of Y began to affect the Z_{peak}, resulting in a decrease in sensitivity. In this way, the balance between d and q determined the suppression of the decrease in sensitivity.

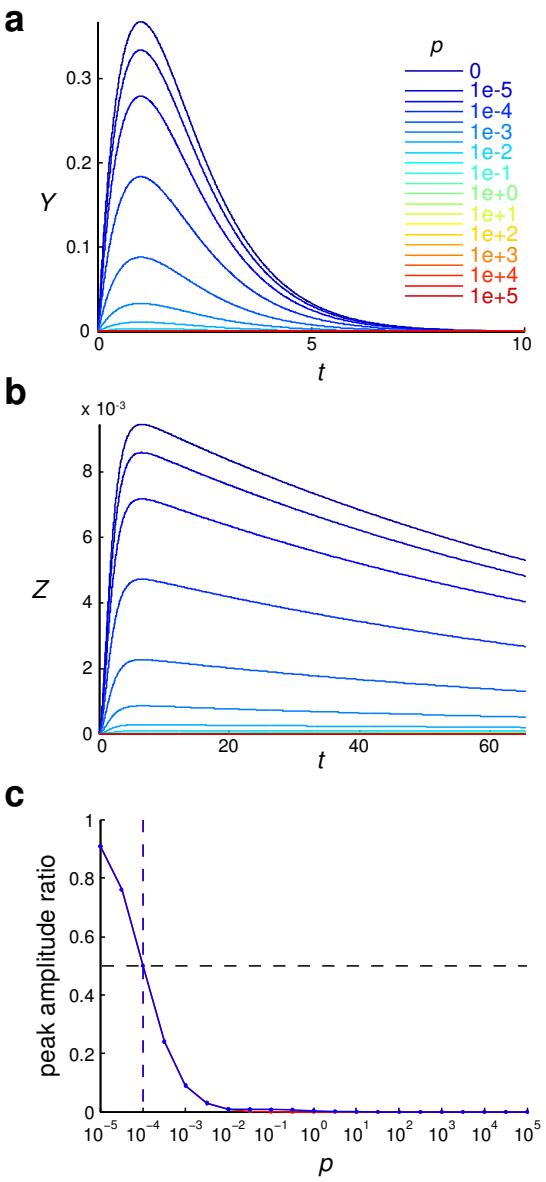

Supplementary Figure S6 | The decrease in the sensitivity to an inhibitor was suppressed when *q* was small. (**a** and **b**) Time courses of *Y* and *Z*, respectively, for the indicated range of *p*. The inset in **a** indicates the value of *p*. *q* was changed to 0.0001 from Fig. 5b,c. (**c**) Dose-response curve for Y_{peak} (red line) and Z_{peak} (blue line) for the inhibitor. Changing the value of *p* can be regarded as changing the concentration of the inhibitor. Y_{peak} and Z_{peak} were normalized according to the maximal responses.

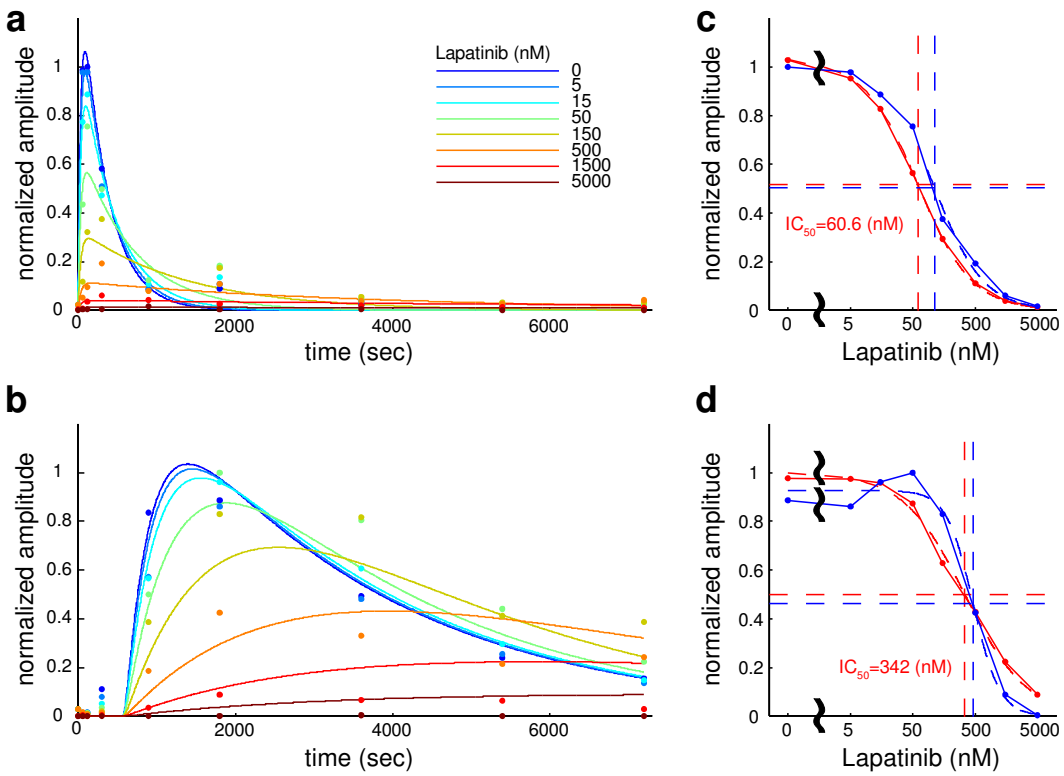

Supplementary Figure S7 | The inhibitor model was capable of reproducing the experimental data. (**a** and **b**) Time courses of *Y* and *Z*, respectively, in the inhibitor model (lines) and in experiments (points). The inhibitor, *Y* and *Z* in the inhibitor model corresponded to lapatinib, phosphorylated Akt and S6, respectively, and the parameters for the inhibitor model were fitted using the experimental data (see Supplementary Note 1). The inhibitor concentrations are shown in the inset. The time courses of *Y* and *Z* successfully reproduced those of phosphorylated Akt and S6, respectively. (**c** and **d**) Dose-response curves of Y_{peak} and Z_{peak}, respectively. Y_{peak} and Z_{peak} in the inhibitor model (red solid line) were fitted using a sigmoid curve (red dashed line). The blue lines show the peak amplitude of phosphorylated Akt (**c**) and S6 (**d**) in the experimental data. The IC_{50} for Y_{peak} was about 61 nM, and the IC_{50} for Z_{peak} was about 342 nM, which was 5.6 times higher than that of Y_{peak}. These values were very similar to the experimental data, suggesting that the decrease in the IC_{50} observed in the experiment was caused by the consecutive first-order reaction.

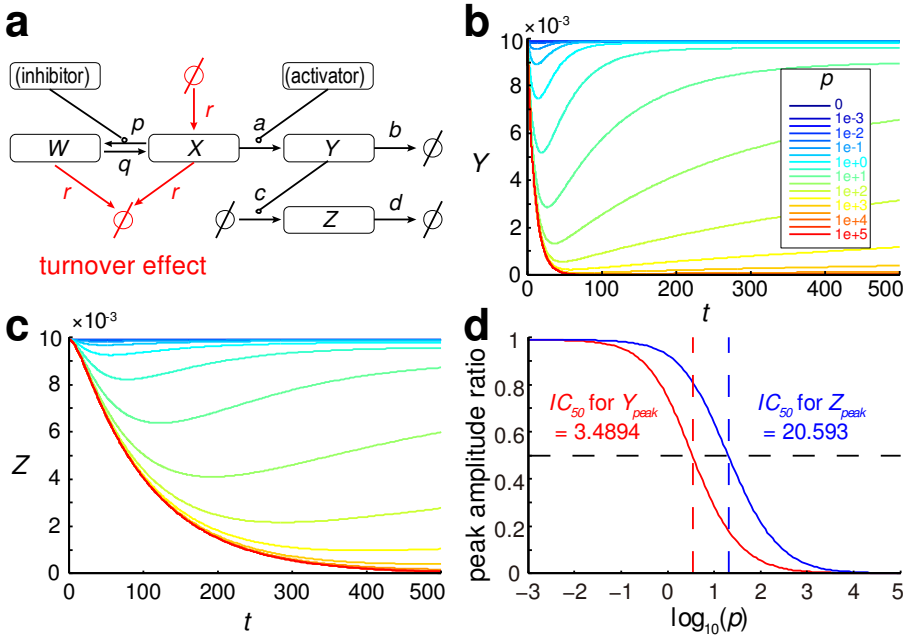

Supplementary Figure S8 | The downstream molecule is less sensitive to an inhibitor than the upstream molecule under physiological-like conditions. (**a**) *In vivo* inhibitor model. The *in vivo* inhibitor model was created by adding turnover reactions to the inhibitor model, while the maintaining the same relation between *Y* and *Z* (see Methods and Supplementary Note 1). The *in vivo* inhibitor model had a new rate constant, *r*, corresponding to the synthesis and degradation rate constants of *X*. The turnover reactions for *X* are needed for constitutive activation. The notations are the same as in Fig. 1b. (**b** and **c**) Time courses of *Y* (**b**) and *Z* (**c**) in response to the indicated *p* (see inset). Note that *p* can be regarded as the concentration of the inhibitor. The addition of the inhibitor resulted in a transient decrease in both *Y* and *Z*. Both Y_{peak} and Z_{peak} decreased as *p* increased. Note that here Y_{peak} and Z_{peak} denoted the decreased peak and the lowest value. The values for *a*, *b*, *c*, *d*, *q*, and *r* were set at 0.1, 0.1, 0.01, 0.01, 1 and 0.0001, respectively. The activator was administered and reached an equilibrium before inhibition. (**d**) Dose-response curves of Y_{peak} (red line) and Z_{peak} (blue line) for the inhibitor. The dashed lines indicate the IC_{50} values for Y_{peak} and Z_{peak}. The IC_{50} for Y_{peak} was 3.49 and that for Z_{peak} was 20.6, indicating that Z_{peak} was less sensitive to the inhibitor than Y_{peak} under physiological-like conditions. The maximal values of Y_{peak} and Z_{peak} were normalized to 1.

Supplementary Table S1. Decoupling conditions. The time courses Y_1 and Y_2 have the parameters (a_1, b_1) and (a_2, b_2), respectively. The decoupling effect is defined as $Y_{peak}(1) > Y_{peak}(2)$ and $Z_{peak}(1) < Z_{peak}(2)$. The parameters are classified in Areas I to III, and the conditions for the decoupling effect are listed as follows. Some conditions are written in simple form using equation (S24). All the conditions have the relationship of $\frac{a_1}{b_1} > \frac{a_2}{b_2}$ [1], which comes from $Y_{peak}(1) > Y_{peak}(2)$. A contradiction can be noted in the conditions (1), (2), (3), and (8), indicating that the decoupling effect cannot occur under these conditions.

Cond. No.	Parameter area		$Z_{peak}(1) < Z_{peak}(2)$	Parameters (1)		Parameters (2)	
	(a_1, b_1)	(a_2, b_2)	[2]	[3]	[4]	[5]	[6]
(1)	Area I	Area I	$\frac{a_1}{b_1} < \frac{a_2}{b_2}$	$a_1 < d$	$b_1 < d$	$a_2 < d$	$b_2 < d$
(2)	Area I	Area II	$\frac{a_1}{b_1} < \frac{d}{b_2}$	$a_1 < d$	$b_1 < d$	$a_2 > d$	$a_2 > b_2$
(3)	Area I	Area III	$\left(\frac{a_1}{b_1}\right)^{\frac{1}{1-a_1/b_1}} < \frac{a_2}{b_2}\left(\frac{d}{a_2}\right)^{\frac{1}{1-d/a_2}}$	$a_1 < d$	$b_1 < d$	$b_2 > d$	$a_2 < b_2$
(4)	Area II	Area I	$\frac{d}{b_1} < \frac{a_2}{b_2}$	$a_1 > d$	$a_1 > b_1$	$a_2 < d$	$b_2 < d$
(5)	Area II	Area II	$\frac{d}{b_1} < \frac{d}{b_2}$	$a_1 > d$	$a_1 > b_1$	$a_2 > d$	$a_2 > b_2$
(6)	Area II	Area III	$\left(\frac{d}{b_1}\right)^{\frac{1}{1-d/b_1}} < \frac{a_2}{b_2}\left(\frac{d}{a_2}\right)^{\frac{1}{1-d/a_2}}$	$a_1 > d$	$a_1 > b_1$	$b_2 > d$	$a_2 < b_2$
(7)	Area III	Area I	$\frac{a_1}{b_1}\left(\frac{d}{a_1}\right)^{\frac{1}{1-d/a_1}} < \left(\frac{a_2}{b_2}\right)^{\frac{1}{1-a_2/b_2}}$	$b_1 > d$	$a_1 < b_1$	$a_2 < d$	$b_2 < d$
(8)	Area III	Area II	$\frac{a_1}{b_1}\left(\frac{d}{a_1}\right)^{\frac{1}{1-d/a_1}} < \left(\frac{d}{b_2}\right)^{\frac{1}{1-d/b_2}}$	$b_1 > d$	$a_1 < b_1$	$a_2 > d$	$a_2 > b_2$
(9)	Area III	Area III	$\frac{a_1}{b_1}\left(\frac{d}{a_1}\right)^{\frac{1}{1-d/a_1}} < \frac{a_2}{b_2}\left(\frac{d}{a_2}\right)^{\frac{1}{1-d/a_2}}$	$b_1 > d$	$a_1 < b_1$	$b_2 > d$	$a_2 < b_2$

Supplementary Note 1

Consecutive first-order reaction

A consecutive first-order reaction, which is called a low-pass filter in the field of engineering, can be represented as

$$F \xrightarrow{k/\tau} G \xrightarrow{1/\tau} (\phi),$$

where k denotes the gain of the filter and τ denotes the time constant of the filter. The output of the reaction, $G(t)$, is dependent on the input, $F(t)$, and the temporal evolution of $G(t)$ is described by the ordinary differential equation as follows:

$$\tau \frac{dG(t)}{dt} = k \cdot F(t) - G(t). \tag{S1}$$

We obtained an analytical solution for $G(t)$ as follows:

$$G(t) = \frac{k}{\tau} \mathrm{e}^{-\frac{t}{\tau}} \int_{u=0}^{t} F(u) \mathrm{e}^{\frac{u}{\tau}} du.$$

The gain k scales the amplitude of $G(t)$ uniformly but does not affect the shape of the time course of $G(t)$. Therefore, the gain k does not affect the results in the main text.

Activator model

The activator model can be described using the following ordinary differential equations:

$$\begin{cases} \dfrac{dX}{dt} &= -a \cdot X, \\ \dfrac{dY}{dt} &= a \cdot X - b \cdot Y, \\ \dfrac{dZ}{dt} &= c \cdot Y - d \cdot Z, \end{cases} \tag{S2}$$

where parameters a, b, c, and d are the rate constants of the synthesis of Y, the degradation of Y, synthesis of Z, and the degradation of Z, respectively (see Fig. 1b). Comparing the equation of dZ/dt with equation (S1), following relationships were found:

$$\begin{cases} \tau = 1/d, \\ k = c/d. \end{cases}$$

The initial conditions were given as follows:

$$\begin{cases} X(0) &= x, \\ Y(0) &= 0, \\ Z(0) &= 0, \end{cases}$$

and the analytical solution of the equations is

$$\begin{cases} X(t) &= x\mathrm{e}^{-at}, \\ Y(t) &= \dfrac{ax}{b-a}\left(\mathrm{e}^{-at} - \mathrm{e}^{-bt}\right), \\ Z(t) &= \dfrac{-acx\mathrm{e}^{-at}}{(d-a)(a-b)} + \dfrac{-acx\mathrm{e}^{-bt}}{(a-b)(b-d)} + \dfrac{-acx\mathrm{e}^{-dt}}{(b-d)(d-a)}, \end{cases} \tag{S3}$$

where $(a \neq b \neq d)$.

Note that the parameter x scales the amplitudes of all the time coureses uniformly but does not affect the shape of the time coureses. Therefore, the paramter x does not affect the results in the main text, and we set $x = 1$ unless otherwise specified.

Y and Z were regarded as amounts of activated upstream and downstream molecules of a signaling pathway, respectively. In this study, we focused on the relationships between Y and Z, and therefore the biological meaning of X was not specified. We changed the time course of Y by changing a and b, and examined the response of Zpeak in main text.

We can introduce more detailed expression of the activator model using $\hat{a}$,

$$\begin{cases} \dfrac{dX}{dt} &= -a \cdot X, \\ \dfrac{dY}{dt} &= \hat{a} \cdot X - b \cdot Y, \\ \dfrac{dZ}{dt} &= c \cdot Y - d \cdot Z, \end{cases}$$

and then obtained the analytical solutions as

$$\begin{cases} X(t) &= x\mathrm{e}^{-at}, \\ Y(t) &= \dfrac{\hat{a}x}{b-a}\left(\mathrm{e}^{-at}-\mathrm{e}^{-bt}\right), \\ Z(t) &= \dfrac{-\hat{a}cx\mathrm{e}^{-at}}{(d-a)(a-b)}+\dfrac{-\hat{a}cx\mathrm{e}^{-bt}}{(a-b)(b-d)}+\dfrac{-\hat{a}cx\mathrm{e}^{-dt}}{(b-d)(d-a)}. \end{cases}$$

Thus, the paramter $\hat{a}$ scales the amplitudes of time coureses of Y and Z uniformly but does not affect the shape of the time coureses. Therefore, the paramter $\hat{a}$ does not affect the results in the main text, and we set $\hat{a}=a$ in this study.

Peak time and peak amplitude of the activator model

The time course of Y has a peak at the peak time t_Y, and t_Y is given by the solution of the equation:

$$\begin{aligned} \frac{dY}{dt} &= \frac{a}{b-a}\left(-a\mathrm{e}^{-at_Y}+b\mathrm{e}^{-bt_Y}\right) \\ &= 0, \end{aligned} \tag{S4}$$

hence,

$$t_Y = \frac{\log\left(\dfrac{a}{b}\right)}{a-b} \tag{S5}$$

and from equation (S3), the peak amplitude Y_{peak} can be obtained,

$$\begin{aligned} Y_{peak} &= Y(t_Y) \\ &= \frac{a}{b-a}\left\{\left(\frac{a}{b}\right)^{\frac{-a}{a-b}}-\left(\frac{a}{b}\right)^{\frac{-b}{a-b}}\right\} \\ &= \frac{a}{b-a}\left(\frac{a}{b}\right)^{\frac{-b}{a-b}}\left\{\left(\frac{a}{b}\right)^{\frac{b-a}{a-b}}-1\right\} \end{aligned}$$

$$= \frac{a}{b-a}\left(\frac{a}{b}\right)^{\frac{-b}{a-b}}\left\{\frac{b}{a}-1\right\}$$

$$= \left(\frac{a}{b}\right)^{\frac{-b}{a-b}}$$

$$= \left(\frac{a}{b}\right)^{\frac{1}{1-a/b}}. \tag{S6}$$

Next, we assumed that the time course of Z has a single peak (Z_{peak}) at $t = t_Z$. t_Z is given by the solution of the equation $dZ(t_Z)/dt = 0$. But the equation $dZ/dt = 0$ is difficult to solve for t. Therefore, we introduced an approximation of Z using the symmetry and singularity of Z, and divided the parameter space as follows:

$$\begin{cases} \text{A}rea\ I & : a < d \text{ a}nd\ b < d \\ \text{A}rea\ II & : a > d \text{ a}nd\ a > b \\ \text{A}rea\ III & : b > d \text{ a}nd\ a < b. \end{cases} \tag{S7}$$

In area I, we introduced a new parameter, h, as $d = a/h$. From equation (S7),

$$\begin{cases} a < d & \Rightarrow h < 1 \\ b < d & \Rightarrow \dfrac{bh}{a} < 1 \end{cases} \tag{S8}$$

and from equation (S3),

$$Z(t) = \frac{-ac\mathrm{e}^{-at}}{(\frac{a}{h}-a)(a-b)} + \frac{-ac\mathrm{e}^{-bt}}{(a-b)(b-\frac{a}{h})} + \frac{-ac\mathrm{e}^{-\frac{a}{h}t}}{(b-\frac{a}{h})(\frac{a}{h}-a)}$$

$$= \frac{h}{a}\left\{\frac{-ac\mathrm{e}^{-at}}{(1-h)(a-b)} + \frac{ac\mathrm{e}^{-bt}}{(a-b)(1-\frac{bh}{a})} + \frac{ch\mathrm{e}^{-\frac{a}{h}t}}{(1-\frac{bh}{a})(1-h)}\right\}.$$

The Maclaurin series expansion for the above equation under the conditions in (S8) is

given by,

$$Z(t) = \frac{h}{a}\left\{\frac{-ace^{-at}}{(a-b)}\cdot\sum_{k=0}^{\infty}h^k + \frac{ace^{-bt}}{(a-b)}\cdot\sum_{k=0}^{\infty}\left(\frac{bh}{a}\right)^k + ch\cdot\sum_{k=0}^{\infty}h^k\cdot\sum_{l=0}^{\infty}\left(\frac{bh}{a}\right)^l\cdot\sum_{m=0}^{\infty}\frac{1}{m!}\left(\frac{-at}{h}\right)^m\right\}$$

$$= \frac{h}{a}\left\{\frac{-ace^{-at}}{(a-b)} + \frac{-ace^{-at}}{(a-b)}\cdot\sum_{k=1}^{\infty}h^k + \frac{ace^{-bt}}{(a-b)} + \frac{ace^{-bt}}{(a-b)}\cdot\sum_{k=1}^{\infty}\left(\frac{bh}{a}\right)^k + c\cdot\sum_{k=1}^{\infty}h^k\cdot\sum_{l=0}^{\infty}\left(\frac{bh}{a}\right)^l\cdot\sum_{m=0}^{\infty}\frac{1}{m!}\left(\frac{-at}{h}\right)^m\right\}$$

$$= \frac{h}{a}\left\{\frac{ac}{(b-a)}\left(e^{-at} - e^{-bt}\right) + O(h)\right\}$$

$$\approx \frac{ac}{d(b-a)}\left(e^{-at} - e^{-bt}\right)$$

$$= \frac{c}{d}\cdot\frac{a}{(b-a)}\left(e^{-at} - e^{-bt}\right). \tag{S9}$$

In Area I, the approximation of Z using equation (S9) is equal to Y (equation (S3)) without scaling factor c/d, hence,

$$t_Z = \frac{\log\left(\frac{a}{b}\right)}{a-b} \tag{S10}$$

$$Z_{peak} = \frac{c}{d}\left(\frac{a}{b}\right)^{\frac{1}{1-a/b}}. \tag{S11}$$

In area II, we set the parameter h as $a = d/h$. From equation (S7),

$$\begin{cases} a > d & \Rightarrow h < 1 \\ a > b & \Rightarrow \dfrac{bh}{d} < 1 \end{cases} \tag{S12}$$

and from equation (S3),

$$Z(t) = \frac{-\frac{d}{h}\cdot c\cdot \mathrm{e}^{-\frac{d}{h}t}}{(d-\frac{d}{h})(\frac{d}{h}-b)} + \frac{-\frac{d}{h}\cdot c\cdot \mathrm{e}^{-bt}}{(\frac{d}{h}-b)(b-d)} + \frac{-\frac{d}{h}\cdot c\cdot \mathrm{e}^{-dt}}{(b-d)(d-\frac{d}{h})}$$

$$= \frac{\frac{h}{d}\cdot c\cdot \mathrm{e}^{-\frac{d}{h}t}}{(1-h)(1-\frac{bh}{d})} + \frac{-c\mathrm{e}^{-bt}}{(1-\frac{bh}{d})(b-d)} + \frac{c\mathrm{e}^{-dt}}{(b-d)(1-h)}.$$

The Maclaurin series expansion for the above equation under the conditions in (S12) is given by,

$$Z(t) = \frac{ch}{d}\cdot\sum_{k=0}^{\infty}h^k\cdot\sum_{l=0}^{\infty}\left(\frac{bh}{d}\right)^l\cdot\sum_{m=0}^{\infty}\frac{1}{m!}\left(\frac{-dt}{h}\right)^m + \frac{-c\mathrm{e}^{-bt}}{(b-d)}\cdot\sum_{k=0}^{\infty}\left(\frac{bh}{d}\right)^k + \frac{c\mathrm{e}^{-dt}}{(b-d)}\cdot\sum_{k=0}^{\infty}h^k$$

$$= \frac{c}{d}\cdot\sum_{k=1}^{\infty}h^k\cdot\sum_{l=0}^{\infty}\left(\frac{bh}{d}\right)^l\cdot\sum_{m=0}^{\infty}\frac{1}{m!}\left(\frac{-dt}{h}\right)^m + \frac{-c\mathrm{e}^{-bt}}{(b-d)} + \frac{-c\mathrm{e}^{-bt}}{(b-d)}\cdot\sum_{k=1}^{\infty}\left(\frac{bh}{d}\right)^k + \frac{c\mathrm{e}^{-dt}}{(b-d)} + \frac{c\mathrm{e}^{-dt}}{(b-d)}\cdot\sum_{k=1}^{\infty}h^k$$

$$= \frac{c}{(b-d)}\left(\mathrm{e}^{-dt}-\mathrm{e}^{-bt}\right)+O(h)$$

$$\approx \frac{c}{(b-d)}\left(\mathrm{e}^{-dt}-\mathrm{e}^{-bt}\right)$$

$$= \frac{c}{d}\cdot\frac{d}{(b-d)}\left(\mathrm{e}^{-dt}-\mathrm{e}^{-bt}\right). \tag{S13}$$

In Area II , we have

$$t_Z = \frac{\log\left(\frac{d}{b}\right)}{d-b} \tag{S14}$$

$$Z_{peak} = \frac{c}{d}\left(\frac{d}{b}\right)^{\frac{1}{1-d/b}}. \tag{S15}$$

In area III , we set the parameter h as $b = d/h$. From equation (S7),

$$\begin{cases} b > d & \Rightarrow h < 1 \\ a < b & \Rightarrow \dfrac{ah}{d} < 1 \end{cases} \tag{S16}$$

and from equation (S3),

$$Z(t) = \frac{-ace^{-at}}{(d-a)(a-\frac{d}{h})} + \frac{-ace^{-\frac{d}{h}t}}{(a-\frac{d}{h})(\frac{d}{h}-d)} + \frac{-ace^{-dt}}{(\frac{d}{h}-d)(d-a)}$$

$$= \frac{h}{d}\left\{ \frac{ace^{-at}}{(d-a)(1-\frac{ah}{d})} + \frac{\frac{h}{d}\cdot ace^{-\frac{d}{h}t}}{(1-\frac{ah}{d})(1-h)} + \frac{-ace^{-dt}}{(1-h)(d-a)} \right\}.$$

The Maclaurin series expansion for the above equation under the conditions in (S16) is given by,

$$Z(t) = \frac{h}{d}\left\{ \frac{ace^{-at}}{(d-a)} \cdot \sum_{k=0}^{\infty}\left(\frac{ah}{d}\right)^k + \frac{ach}{d} \cdot \sum_{k=0}^{\infty} h^k \cdot \sum_{l=0}^{\infty}\left(\frac{ah}{d}\right)^l \cdot \sum_{m=0}^{\infty}\frac{1}{m!}\left(\frac{-dt}{h}\right)^m + \frac{-ace^{-dt}}{(d-a)} \cdot \sum_{k=0}^{\infty} h^k \right\}$$

$$= \frac{h}{d}\left\{ \frac{ace^{-at}}{(d-a)} + \frac{ace^{-at}}{(d-a)} \cdot \sum_{k=1}^{\infty}\left(\frac{ah}{d}\right)^k + \frac{ac}{d} \cdot \sum_{k=1}^{\infty} h^k \cdot \sum_{l=0}^{\infty}\left(\frac{ah}{d}\right)^l \cdot \sum_{m=0}^{\infty}\frac{1}{m!}\left(\frac{-dt}{h}\right)^m \right.$$
$$\left. + \frac{-ace^{-dt}}{(d-a)} + \frac{-ace^{-dt}}{(d-a)} \cdot \sum_{k=1}^{\infty} h^k \right\}$$

$$= \frac{h}{d}\left\{ \frac{ac}{(d-a)}\left(e^{-at} - e^{-dt}\right) + O(h) \right\}$$

$$\approx \frac{1}{b} \cdot \frac{ac}{(a-d)}\left(e^{-dt} - e^{-at}\right)$$

$$= \frac{ac}{bd} \cdot \frac{d}{(a-d)}\left(e^{-dt} - e^{-at}\right). \tag{S17}$$

In Area III , we have

$$t_Z = \frac{\log\left(\frac{d}{a}\right)}{d-a} \tag{S18}$$

$$Z_{peak} = \frac{ac}{bd}\left(\frac{d}{a}\right)^{\frac{1}{1-d/a}}. \tag{S19}$$

In summary, the approximations for $Z(t), t_Z$, and Z_{peak} in Areas I, II , and III are as follows:

$$Z(t) \approx \begin{cases} \frac{c}{d}\cdot\frac{a}{(b-a)}\left(\mathrm{e}^{-at}-\mathrm{e}^{-bt}\right) & (\text{Area I}: a<d, b<d) \\ \frac{c}{d}\cdot\frac{d}{(b-d)}\left(\mathrm{e}^{-dt}-\mathrm{e}^{-bt}\right) & (\text{Area II}: a>d, a>b) \\ \frac{ac}{bd}\cdot\frac{d}{(a-d)}\left(\mathrm{e}^{-dt}-\mathrm{e}^{-at}\right) & (\text{Area III}: b>d, a<b) \end{cases},$$

$$t_Z \approx \begin{cases} \frac{\log\left(\frac{a}{b}\right)}{a-b} & (\text{Area I}: a<d, b<d) \\ \frac{\log\left(\frac{d}{b}\right)}{d-b} & (\text{Area II}: a>d, a>b) \\ \frac{\log\left(\frac{d}{a}\right)}{d-a} & (\text{Area III}: b>d, a<b) \end{cases},$$

$$Z_{peak} \approx \begin{cases} \dfrac{c}{d}\left(\dfrac{a}{b}\right)^{\frac{1}{1-a/b}} & (\text{Area I}: a < d, b < d) \\ \dfrac{c}{d}\left(\dfrac{d}{b}\right)^{\frac{1}{1-d/b}} & (\text{Area II}: a > d, a > b) \\ \dfrac{ac}{bd}\left(\dfrac{d}{a}\right)^{\frac{1}{1-d/a}} & (\text{Area III}: b > d, a < b) \end{cases} .$$

It should be noted that these approximations become closer to the numerical value if the parameter h becomes smaller than 1, where the parameter set is far from the boundaries of the areas. Each approximation of t_Z and Z_{peak} is equal to each other at the boundaries of the areas.

Note that the term $\frac{c}{d}$ $(=k)$ scales approximated $Z(t)$ and Z_{peak} in all the three areas uniformly. Therefore, E was defined in main text as

$$E = \frac{1}{k} \cdot \frac{Z_{peak}}{Y_{peak}}. \tag{S20}$$

A function included in the peak amplitudes increases strictly monotonically

Y_{peak} and Z_{peak} are represented by the form

$$A \cdot f(u),$$

where

$$f(u) = u^{\frac{1}{1-u}}. \tag{S21}$$

For example, Z_{peak} in area I, $A = c/d$ and $u = a/b$.

Here, we show that $f(u)$ is a strictly monotonically increaseing function where

$u > 0$. The derivative of $f(u)$ is

$$\frac{df(u)}{du} = \frac{u\log(u) - (u-1)}{u(u-1)^2} \cdot u^{\frac{1}{1-u}}. \tag{S22}$$

Because $u(u-1)^2 > 0$ at $u \neq 1$ and $u^{\frac{1}{1-u}} > 0$, we show

$$g(u) = u\log(u) - (u-1) > 0,$$

where $u \neq 1$.

The derivative of the function g(u) is

$$\frac{dg(u)}{du} = \log(u),$$

$$= \begin{cases} < 0 & (0 < u < 1), \\ = 0 & (u = 1), \\ > 0 & (u > 1), \end{cases}$$

and,

$$g(1) = 1 \cdot \log(1) - (1-1)$$

$$= 0.$$

Therefore, $g(u) > 0$ where $u > 0$ and $u \neq 1$. This result proves that the function $f(u)$ increases monotonically where for $u > 0$ and $u \neq 1$.

If $u = 1$, we have

$$\frac{df(1)}{du} = \frac{0}{0} \cdot 1^{\frac{1}{0}},$$

which includes two indeterminate forms. Applying L'Hospital's rule twice we have

$$
\begin{aligned}
\lim_{u\to 1}\frac{df(u)}{du} &= \lim_{u\to 1}\frac{\frac{d}{du}\left(u\log(u)-(u-1)\right)}{\frac{d}{du}u(u-1)^2}\cdot\lim_{u\to 1}u^{\frac{1}{1-u}} \\
&= \lim_{u\to 1}\frac{\log(u)}{(3u-1)(u-1)}\cdot\frac{1}{e} \\
&= \lim_{u\to 1}\frac{\frac{d}{du}\log(u)}{\frac{d}{du}(3u-1)(u-1)}\cdot\frac{1}{e} \\
&= \lim_{u\to 1}\frac{\frac{1}{u}}{6u-4}\cdot\frac{1}{e} \\
&= \frac{1}{2e} \\
&> 0,
\end{aligned}
$$

where

$$
\begin{aligned}
\lim_{u\to 1}u^{\frac{1}{1-u}} &= \lim_{v\to 0}\left(1-\frac{1}{v}\right)^{\frac{1}{1-\left(1-\frac{1}{v}\right)}} \\
&= \lim_{v\to 0}\left(1-\frac{1}{v}\right)^{-v} \\
&= \frac{1}{e}.
\end{aligned}
$$

This result proves that $f(u)$ is increasing function at $u=1$.

In summary, we obtained

$$
\frac{df(u)}{du}>0 \tag{S23}
$$

where $u>0$, and we found that the function $f(u)$ increases strictly monotonically for $u>0$. Consequently we have

$$
\begin{cases} f(u_1)>f(u_2)\Leftrightarrow u_1>u_2 \\ f(u_1)<f(u_2)\Leftrightarrow u_1<u_2 \end{cases} \tag{S24}
$$

We used this relationships in Supplementary Table S1. The function f is indicated

in Supplementary Fig. S1b as $Y_{peak} = f(a/b)$.

Estimation of signal transfer efficiency from peak times

The signal transfer efficiency E was defined in main text as

$$E = \frac{1}{k} \cdot \frac{Z_{peak}}{Y_{peak}},$$

where $k = c/d$, which means the gain.

In area I, the signal transfer efficiency E is 1 because the approximation of Z_{peak} is equal to $k \cdot Y_{peak}$.

In area II,

$$E = \frac{\frac{c}{d}\left(\frac{d}{b}\right)^{\frac{b}{b-d}}}{k\left(\frac{a}{b}\right)^{\frac{b}{b-a}}}$$

$$= \frac{\exp\left(\frac{-b}{d-b}\log\left(\frac{d}{b}\right)\right)}{\exp\left(\frac{-b}{a-b}\log\left(\frac{a}{b}\right)\right)}$$

$$= \frac{\exp(-b \cdot t_Z)}{\exp(-b \cdot t_Y)}$$

$$= \exp(-b(t_Z - t_Y)).$$

In area III,

$$E = \frac{\frac{ac}{bd}\left(\frac{d}{a}\right)^{\frac{a}{a-d}}}{k\left(\frac{a}{b}\right)^{\frac{b}{b-a}}}$$

$$= \frac{\left(\frac{d}{a}\right)^{\frac{a}{a-d}}}{\left(\frac{a}{b}\right)^{\frac{b}{b-a}-1}}$$

$$= \frac{\left(\frac{d}{a}\right)^{\frac{a}{a-d}}}{\left(\frac{a}{b}\right)^{\frac{a}{b-a}}}$$

$$= \frac{\exp\left(\frac{-a}{d-a}\log\left(\frac{d}{a}\right)\right)}{\exp\left(\frac{-a}{a-b}\log\left(\frac{a}{b}\right)\right)}$$

$$= \frac{\exp(-a \cdot t_Z)}{\exp(-a \cdot t_Y)}$$

$$= \exp(-a(t_Z - t_Y)).$$

In summary,

$$E = \begin{cases} 1 & (\mathrm{A}reaI) \\ \exp(-b\Delta t) & (\mathrm{A}reaII) \\ \exp(-a\Delta t) & (\mathrm{A}reaIII) \end{cases} \tag{S25}$$

where $\Delta t = t_Z - t_Y$.

We summarized these equations and found that the conditions for area II include $a > b$ and that the coefficient is the smaller value, b. In other words, the coefficient of Δt

is a or b, whichever is smaller. The conditions for area III include $b > a$, and the coefficient is the smaller value, a. Therefore we introduced a similar coefficient as follows:

$$E = \exp\left(\frac{-ab}{a+b}\Delta t\right). \tag{S26}$$

We estimated the value of E from the equation in (S25) and the numerical value of Δt. We compared the estimated E to the numerical value of E and found that the difference in the estimation was more than 80% around the borders of areas II and III. We also found that using equation (S26) instead of (S25) improved the error near the border.

Parameter estimation of the activator model and selection of experimental data sets for validation of the attenuation property of signal transfer efficiency

The parameters of the activator model were estimated using experimental data (Supplementary data 1) according to two methods in series. First, a meta-evolutionary programming method was used to approach the neighborhood of the local minimum. Second, the Nelder-Mead method was used to reach the local minimum. Using these methods, the parameters were estimated to minimize the objective function value, which was defined as the sum of the square residuals between our measurements and the model trajectories.

We made two minor modifications to the activator model as follows. First, the output of the low-pass filter $(Z(t))$ was given a delay time l because some downstream molecule of the pathway, the experimental counterpart of $Z(t)$, seemed to have a delay time. Accordingly, $Z(t)$ was modified to $Z(t-l)$, and $Z(t-l)$ was set as 0 at $t < l$. Second, the parameter a, b and x can have different and arbitrary values for respective time courses in a pathway. Please note that other parameters (c, d and l) could have a common value for respective time courses in a pathway. In other words, if we have 6 sets of experimental time course from a single pathway, the 21 paramters (a_1 ~ a_6, b_1 ~ b_6, c, d, l, and x_1 ~ x_6) were estimated at once. These modification satisfyes the conditions (a) and (b) but not for condition (c) shown in Disucussion.

There may be some interplay between the signalling dynamics and the ability to estimate parameters. However, our modeling framework is suitable for the analysis of transient time courses, and time courses of our experimental data are almost transient. Therefore, the parameters were correctly estimated by these data sets.

After 200 independent estimations, we selected the model with the minimum objective function value. The estimated parameters are shown in supplementary data , and the time courses of the estimated model are shown in supplemental data.

In the selected model, we calculated normalized RSS as follows and we excluded the set of the time course whose model does not satisfy any of the following inequations:

$$normalized\_RSS_i^{upstream} = \frac{\sum_{j=1}^{m}(Y(t_j|a_i,b_i,c,d,l,x_i) - measurement_i^{upstream}(t_j))^2}{\sum_{j=1}^{m}(measurement_i^{upstream}(t_j))^2} < 0.1,$$

$$normalized\_RSS_i^{downstream} = \frac{\sum_{j=1}^{m}Z(t_j|a_i,b_i,c,d,l,x_i) - measurement_i^{downstream}(t_j))^2}{\sum_{j=1}^{m}(measurement_i^{downstream}(t_j))^2} < 0.1,$$

$$normalized\_RSS_{all}^{upstream} = \frac{\sum_{i=1}^{n}\sum_{j=1}^{m}(Y(t_j|a_i,b_i,c,d,l,x_i) - measurement_i^{upstream}(t_j))^2}{\sum_{i=1}^{n}\sum_{j=1}^{m}(measurement_i^{upstream}(t_j))^2} < 0.3,$$

$$normalized\_RSS_{all}^{downstream} = \frac{\sum_{i=1}^{n}\sum_{j=1}^{m}Z(t_j|a_i,b_i,c,d,l,x_i) - measurement_i^{downstream}(t_j))^2}{\sum_{i=1}^{n}\sum_{j=1}^{m}(measurement_i^{downstream}(t_j))^2} < 0.3,$$

where i and j represents the doses and the time points, respectively. We confirmed that choice of the cutoff values for normalized RSS has little effect on our results. We also excluded the inhbitor experiments and the set of the time courses whose duration of upstream signal ($t_{1/2}$) or peak amplitudes coud not be obtained by experiment because of sustained response or nonresponsive to the stimuli. We selected the rest of the time courses which satisfy the conditions (a) and (b), and analyzed their experimental data for Figure 3. $t_{1/2}$ was obtained by linear interpolation of the experimental time course of the upstream molecule. The time constant of the pathway τ was obtained as $1/d$ of the model. The signal transfer efficiency (E) was obtained from the ratio of the peak amplitudes of the experimenatl time courses and then divided by $k = c/d$ of the model. Then E was plotted against $\frac{t_{1/2}}{\tau}$ with

the theoretical line in Figure 3 (for derivation of the theoretical line, see Fig. S3).

Proof of EC_{50} decrease in the activator model

We already found that $f(u) = u^{\frac{1}{1-u}}$ for $u > 0$ is strictly monotonically increasing function (equation (S23)). In this section, we show other three characteristics of $f(u)$ and then proof of EC_{50} decrease in the activator model. We also show the relationships between sensitivity increase index (S_i) and the negative regulation of the pathway (d).

First, we show $0 < f(u) < 1$. For limit on $u \to 0$, we have

$$\begin{aligned}\lim_{u\to 0} f(u) &= (0)^{\frac{1}{1-0}} \\ &= 0.\end{aligned}$$

For limit on $u \to \infty$, applying L'Hospital's rule we have

$$\begin{aligned}\lim_{u\to\infty} f(u) &= \lim_{u\to\infty} u^{\frac{1}{1-u}} \\ &= \exp\left(\lim_{u\to\infty} \frac{\log u}{1-u}\right) \\ &= \exp\left(\lim_{u\to\infty} \frac{\frac{d}{du}\log u}{\frac{d}{du}(1-u)}\right) \\ &= \exp\left(\lim_{u\to\infty} \frac{\frac{1}{u}}{-1}\right) \\ &= \exp(0) \\ &= 1\end{aligned}$$

From these results and equation (S23), we found

$$0 < f(u) < 1 \tag{S27}$$

Second, we show $\frac{1}{u}\cdot f(u) = f(1/u)$. We have

$$\begin{aligned}\frac{1}{u}\cdot f(u) &= \frac{1}{u}\cdot u^{\frac{1}{1-u}} \\ &= u^{\frac{1}{1-u}-1} \\ &= u^{\frac{u}{1-u}} \\ &= \left(\frac{1}{u}\right)^{\frac{u}{u-1}} \\ &= \left(\frac{1}{u}\right)^{\frac{1}{1-1/u}} \\ &= f(1/u).\end{aligned}$$

Then we found

$$\frac{1}{u}\cdot f(u) = f(1/u). \tag{S28}$$

Third, we show that the solution of $f(u) = \frac{1}{2}$ is $u = 2$. We have

$$\begin{aligned}f(2) &= (2)^{\frac{1}{1-2}} \\ &= (2)^{-1} \\ &= \frac{1}{2}.\end{aligned}$$

Together with strictly monotonically increasing characteristics of $f(u)$ (equation (S23)), we found

$$f(u) = \frac{1}{2} \Leftrightarrow u = 2. \tag{S29}$$

Finally, we prove the decrease of EC_{50} in the downstream molecule of the activator model. EC_{50} was defined as the concentration of the activator which induce the 50% of maximum response. In this section, a is regarded as the concentration of the activator.

Consider the EC_{50} of Y_{peak} using analytical solution. From equations (S6) and (S21),

$$\begin{aligned} Y_{peak} &= \left(\frac{a}{b}\right)^{\frac{1}{1-a/b}} \\ &= f\left(\frac{a}{b}\right), \end{aligned}$$

and from equation (S27), we found that maximum response of Y_{peak} is 1. Therefore, at the EC_{50}

$$Y_{peak} = \frac{1}{2}.$$

From equation (S29), we have

$$f\left(\frac{a}{b}\right) = \frac{1}{2} \Rightarrow a = 2b. \tag{S30}$$

Thus, the EC_{50} of Y_{peak} is obtained as $2b$.

Consider the EC_{50} of Z_{peak} using approximated analytical solution.

In Area II, from equation (S15), Z_{peak} should not be affected by a.

In Area I, from equations (S11) and (S21),

$$\begin{aligned} Z_{peak} &= \frac{c}{d}\left(\frac{a}{b}\right)^{\frac{1}{1-a/b}} \\ &= \frac{c}{d} \cdot f\left(\frac{a}{b}\right). \end{aligned}$$

From equation (S23), Z_{peak} monotonically increases for a, and from equation (S7),

expression of Z_{peak} is switched to that for Area II where $a \geq d$. Therefore, the maximum response of Z_{peak} is same as the Z_{peak} in Area II, and

$$\max\left(Z_{peak}\right) = \frac{c}{d}\left(\frac{d}{b}\right)^{\frac{1}{1-d/b}} = \frac{c}{d}\cdot f\left(\frac{d}{b}\right),$$

and at the EC_{50} of Z_{peak}, a should satisfy following equation

$$\frac{c}{d}\cdot f\left(\frac{a}{b}\right) = \frac{1}{2}\cdot\frac{c}{d}\cdot f\left(\frac{d}{b}\right)$$

$$\Rightarrow f\left(\frac{a}{b}\right) = \frac{1}{2}\cdot f\left(\frac{d}{b}\right). \tag{S31}$$

Because Z_{peak} monotonically increases for a (from equation (S23)), the EC_{50} of Z_{peak} reaches the maximum when the right hand side of equation (S31) reaches the maximum. From equation (S27), the maximum of the right hand side is

$$\lim_{\frac{d}{b}\to\infty}\frac{1}{2}\cdot f\left(\frac{d}{b}\right) = \frac{1}{2}. \tag{S32}$$

Therefore, the maximum of the EC_{50} of Z_{peak} is

$$f\left(\frac{a}{b}\right) = \frac{1}{2} \Rightarrow a = 2b, \tag{S33}$$

and is the same as EC_{50} of Y_{peak} (equation (S30)). Thus, it is proved that the EC_{50} of Z_{peak} should be equal or smaller than that of Y_{peak} in Area I.

In Area III, from equations (S19) and (S21),

$$Z_{peak} = \frac{ac}{bd}\left(\frac{d}{a}\right)^{\frac{1}{1-d/a}} = \frac{ac}{bd}\cdot f\left(\frac{d}{a}\right).$$

From equation (S28),

$$Z_{peak} = \frac{c}{b} \cdot \frac{a}{d} \cdot f\left(\frac{d}{a}\right)$$
$$= \frac{c}{b} \cdot f\left(\frac{a}{d}\right).$$

From equation (S23), Z_{peak} monotonically increases for a, and from equation (S7), expression of Z_{peak} is switched to that for Area II where $a \geq b$. Therefore, the maximum response of Z_{peak} is same as the Z_{peak} in Area II, and

$$\max\left(Z_{peak}\right) = \frac{c}{d} \cdot f\left(\frac{d}{b}\right),$$

and at the EC_{50} of Z_{peak}, a should satisfy following equation

$$\frac{c}{b} \cdot f\left(\frac{a}{d}\right) = \frac{1}{2} \cdot \frac{c}{d} \cdot f\left(\frac{d}{b}\right)$$

$$\Rightarrow f\left(\frac{a}{d}\right) = \frac{1}{2} \cdot \frac{b}{d} \cdot f\left(\frac{d}{b}\right).$$

Using equation (S28), we have

$$f\left(\frac{a}{d}\right) = \frac{1}{2} \cdot f\left(\frac{b}{d}\right). \tag{S34}$$

Because Z_{peak} monotonically increases for a (from equation (S23)), the EC_{50} of Z_{peak} reaches the maximum when the right hand side of equation (S31) reaches the maximum. From equation (S27), the maximum of the right hand side is

$$\lim_{\frac{b}{d} \to \infty} \frac{1}{2} \cdot f\left(\frac{b}{d}\right) = \frac{1}{2}. \tag{S35}$$

Therefore, the maximum of the EC_{50} of Z_{peak} is

$$f\left(\frac{a}{d}\right) = \frac{1}{2} \Rightarrow a = 2d. \tag{S36}$$

From equation (S7), $d < b$ in Area III. Therefore, it is proved that the EC_{50} of Z_{peak} should be smaller than the EC_{50} of Y_{peak} (equation (S30)).

Thus, it is proved that the EC_{50} of Z_{peak} should be equal or smaller than that of Y_{peak}.

Additionally, we show the relationships between sensitivity increase index (S_i) and the negative regulation of the pathway (d). In the main text, S_i was defined as

$$S_i = \frac{\text{EC}_{50} \text{ of } Y_{peak}}{\text{EC}_{50} \text{ of } Z_{peak}}. \tag{S37}$$

From figure S1b, we found that $f(u)$ is almost same to its maximum value in $u >> 1$. Therefore, the EC_{50} of Z_{peak} can be approximated by its maximum value,

$$\text{EC}_{50} \text{ of } Z_{peak} \approx \begin{cases} 2b & (d > b), \\ 2d & (d < b). \end{cases} \tag{S38}$$

Together with equations (S30) and (S37), we have

$$S_i \approx \begin{cases} 1 & (d > b), \\ \dfrac{b}{d} & (d < b). \end{cases} \tag{S39}$$

This result means that S_i reaches 1 when d became larger than b, and S_i increases as the inverse of d when d became larger than b. This description is equivalent to the descriptions for Figure 4e. Equations (S30), (S38), and (S39) are shown in figure S4 d, e, and f, respectively. In figure S4g, equation (S39) are compared with numerical results (Figure 4e). We confirmed that the approximation used in equations (S38) and (S39) does not affect the qualitative characteristics of the EC_{50} for Z_{peak} and S_i.

Inhibitor model

The inhibitor model can be described by the ordinary differential equations as follows:

$$\begin{cases} \dfrac{dW}{dt} &= -q \cdot W + p \cdot X \\ \dfrac{dX}{dt} &= q \cdot W - (a+p) \cdot X \\ \dfrac{dY}{dt} &= a \cdot X - b \cdot Y \\ \dfrac{dZ}{dt} &= c \cdot Y - d \cdot Z \end{cases} \tag{S40}$$

where the parameters p and q denote the forward and reverse rate constants of the inhibitor reactions, respectively (see Fig. 5a). The initial conditions were given as follows:

$$\begin{cases} W(0) &= \dfrac{p \cdot x}{p+q} \\ X(0) &= \dfrac{q \cdot x}{p+q} \\ Y(0) &= 0 \\ Z(0) &= 0 \end{cases} \tag{S41}$$

where the parameter x denotes the total initial amount of the sum of X and W.

The analytical solution of the equations is as follows:

$$\begin{cases} W(t) &= \dfrac{px}{(p+q)(\beta-\alpha)}\left(\beta \mathrm{e}^{\alpha t} - \alpha \mathrm{e}^{\beta t}\right) \\ X(t) &= \dfrac{qx}{(p+q)(\beta-\alpha)}\left\{(\beta+a)\mathrm{e}^{\alpha t} - (\alpha+a)\mathrm{e}^{\beta t}\right\} \\ Y(t) &= \dfrac{aqx}{p+q}\left\{\dfrac{(\beta+a)\mathrm{e}^{\alpha t}}{(\beta-\alpha)(\alpha+b)} - \dfrac{(\alpha+a)\mathrm{e}^{\beta t}}{(\beta-\alpha)(\beta+b)} - \dfrac{(\alpha+\beta+a+b)\mathrm{e}^{-bt}}{(\alpha+b)(\beta+b)}\right\} \\ Z(t) &= \dfrac{acqx}{p+q}\left\{\dfrac{(\beta+a)\mathrm{e}^{\alpha t}}{(\beta-\alpha)(\alpha+b)(\alpha+d)} - \dfrac{(\alpha+a)\mathrm{e}^{\beta t}}{(\beta-\alpha)(\beta+b)(\beta+d)}\right. \\ & \quad \left. - \dfrac{(\alpha+\beta+a+b)\mathrm{e}^{-bt}}{(\alpha+b)(\beta+b)(d-b)} + \dfrac{(\alpha+\beta+a+d)\mathrm{e}^{-dt}}{(\alpha+d)(\beta+d)(d-b)}\right\} \end{cases} \tag{S42}$$

where

$$\begin{cases} \alpha &= \dfrac{1}{2}\left(-(p+q+a) + \sqrt{(p+q+a)^2 - 4aq}\right) \\ \beta &= \dfrac{1}{2}\left(-(p+q+a) - \sqrt{(p+q+a)^2 - 4aq}\right) \end{cases}$$

and $\alpha \neq \beta \neq -b \neq -d$.

In the analysis of the inhibitor model (Fig. 5; Supplementary Fig. S5 and S6), the parameter x was set as 1 for convenience and simplicity without a loss of generality.

Parameter estimation of the inhibitor model

The parameters of the inhibitor model were estimated using experimental data (Fig. 6) according to two methods in series as described above.

We made two minor modifications to the inhibitor model as follows. First, the parameter p was scaled according to the inhibitor concentration. Second, the output of the low-pass filter $(Z(t))$ was given a delay time l because pS6, the experimental counterpart of $Z(t)$, seemed to have a delay time. Accordingly, $Z(t)$ was modified to $Z(t-l)$, and $Z(t-l)$ was set as 0 at $t < l$.

After 20 independent estimations, we selected the model with the minimum objective function value. The estimated parameters are

$$\begin{cases} a = 3.126\times10^{-3}\ [\text{sec}^{-1}] \\ b = 2.794\times10^{-2}\ [\text{sec}^{-1}] \\ c = 3.041\times10^{-3} \\ d = 3.466\times10^{-4}\ [\text{sec}^{-1}] \\ p = 3.952\times10^{+1}\ [\text{sec}^{-1}\cdot\text{nM}^{-1}] \\ q = 1.791\times10^{+3}\ [\text{sec}^{-1}] \\ x = 1.252\times10^{+1} \\ l = 5.683\times10^{+2}\ [\text{sec}] \end{cases},$$

where inhibitor concentrations were set as 0, 5, 15, 50, 150, 500, 1500, and 5000 [nM]. The time courses of the estimated model are shown in Supplementary Fig. S7.

In vivo inhibitor model

The *in vivo* inhibitor model can be described using ordinary differential equations as follows:

$$\begin{cases} \dfrac{dW}{dt} &= -(q+r)\cdot W + p\cdot X \\ \dfrac{dX}{dt} &= q\cdot W - (a+p+r)\cdot X + r \\ \dfrac{dY}{dt} &= a\cdot X - b\cdot Y \\ \dfrac{dZ}{dt} &= c\cdot Y - d\cdot Z \end{cases} \tag{S43}$$

where the parameter r denotes the synthesis and degradation rate constants of the turnover reactions of X (see Supplementary Fig. S8a). We assumed that the activator was administered and reached an equilibrium before inhibition and set the initial conditions as follows:

$$\begin{cases} W(0) &= 0 \\ X(0) &= \dfrac{r}{a+r} \\ Y(0) &= \dfrac{a}{b}\cdot\dfrac{r}{(a+r)} \\ Z(0) &= \dfrac{ac}{bd}\cdot\dfrac{r}{(a+r)}. \end{cases} \tag{S44}$$

Supplementary Note 2

Negative regulation

Changing the amount of an activator or inhibitor is a straightforward way of controlling the cellular response. However, controlling the concentrations of activators and inhibitors is not always possible. For example, cells should autonomously control the sensitivity to unexpected external stimuli, such as toxins and pathogens. The mechanism we proposed may be one of the solutions used under such conditions.

Negative regulation can include any type of reaction in a signalling pathway, such as degradation or dephosphorylation, and the rate constants of negative regulation can reflect the amount of an enzyme, such as a protease or phosphatase. Therefore, cells can control the signal transfer efficiency and sensitivities to activators and inhibitors by changing the expression levels of such enzymes. Different expression levels of these enzymes may account for the different sensitivities to activators or inhibitors among individual cells and cell lines. In addition, these enzymes reportedly have strong effects on the temporal patterns of signals and sensitivities to activators[8,12,29-31].

Conditions about the analysis of sensitivity control

Analysing the control of sensitivity to activators and inhibitors, in this study, requires the following three conditions: (a) the pathway of interest can be approximated by a consecutive first-order reaction, (b) the time course of the upstream molecule can be expressed as the sum of two exponential curves, and (c) the dose-dependent time courses of the upstream molecule can be expressed by changing the value of a as the doses of an activator or the value of p as the doses of an inhibitor while other parameters remain fixed (Figs. 4-6). On the contrary, analysing the attenuation of signal transfer efficiency, in this study, requires only the first two conditions (Fig. 3). The sensitivity control reflects the relationship between an activator (or an inhibitor), Y, and Z. In contrast, the attenuation of signal transfer efficiency depends on the relationship between Y and Z but not between an activator (or an inhibitor) and Y. Therefore, the analysis of sensitivity control requires conditions that are more stringent. Condition (a) reflects that the elementary reactions of the pathways are not necessarily exact first-order reactions. For example, the Michaelis–Menten type of enzymatic reaction is not an exact first-order reaction, but it can be approximated by a first-order reaction when the substrate is abundant[32]. Even a signalling pathway involving multistep reactions that are more complex can be approximated by consecutive first-order reactions (Fig. 3)[23]. However, pathways including high-order reactions or feedback effects may not be able to be adequately approximated by a consecutive first-order reaction. Additionally, condition (b) may not be satisfied in pathways that include signalling molecules whose time courses are sustained or oscillate. Condition (c) may not be satisfied when there are high-order reactions between Y and the activator or the inhibitor.

Comparing to previous studies about sensitivity

In this study, we analysed the sensitivity differences in the peak amplitudes in a consecutive first-order reaction. The sensitivity differences in the equilibrium amplitudes have previously been analysed, and the depletion of the substrate in a biochemical reaction has been shown to control the sensitivity[16-18]. For example, consider the phosphorylation and dephosphorylation of a substrate in equilibrium. A kinase is activated by an activator and phosphorylates the substrate; the phosphorylated substrate (product) is then dephosphorylated and returns to being a substrate. The activated kinase and the product can be regarded as the upstream and downstream molecules of the biochemical reaction. Increasing the dose of the activator increases the amount of activated kinase. The substrate is phosphorylated by the activated kinase, and in the presence of an excess of activated kinase, the substrate is consumed and eventually depleted. When the substrate is depleted, further increases in the amount of activator do not increase the amount of product, although the amount of activated kinase is increased. Therefore, the product reaches a plateau before the activated kinase reaches a plateau, and the EC_{50} for the product is smaller than the EC_{50} for the activated kinase when the substrate is depleted. Thus, the depletion of the substrate can induce an increase in sensitivity.

In contrast, when the amount of substrate is not changed, an enzymatic reaction can be approximated by a first-order reaction, as described above. Because the first-order reaction ignores the depletion of the substrate, the consecutive first-order reaction examined in this study is not influenced by the depletion effect. Thus, the mechanism responsible for the control of sensitivity in this study differs from that in previous studies[16-18]. General biochemical reactions, including the Michaelis–Menten type of enzymatic reaction, possess the intrinsic characteristics of both the depletion effect and the attenuation of signal transfer efficiency. Therefore, both characteristics may generally contribute to the control of sensitivity. Reportedly, sensitivity can also be controlled by the characteristics of network motifs, such as a negative feedback loop or an incoherent feed-forward loop[6,10,19,20].

Extent of the attenuation of signal transfer efficiency

The attenuation of signal transfer efficiency may be involved in many cellular processes. For example, the process of gene expression comprises both the synthesis and the degradation (i.e., negative regulation) of the gene product. The synthesis is induced by the activities of upstream signalling molecules, and the degradation of the gene product depends on the actual amount of gene product present. This process can be approximated by a consecutive first-order reaction, where the activities of the upstream signalling molecule and the gene product can be regarded as Y and Z in the activator model, respectively[20,33-35]. In general, the synthesis and degradation rate constants for the time course of the cellular signalling pathway are larger than the degradation rate constant of the gene product[35], suggesting that the

attenuation of signal transfer efficiency can be observed in signalling-dependent gene expression. Indeed, we found that ERK-dependent c-FOS expression could be approximated by a consecutive first-order reaction, and attenuation of signal transfer efficiency was observed (Supplementary Data 2). We could not examine the downstream sensitivity to growth factors of the pathway because EGF-dependent ERK activation did not satisfy condition (c). However, in a signalling pathway that satisfies conditions (a), (b), and (c), the gene product may be more sensitive than the upstream signalling molecule to growth factors. The gene expression system may use this characteristic to increase its sensitivity to growth factors.

The attenuation of signal transfer efficiency should be considered when interpreting experimental data. For example, a luciferase assay system is used as a reporter for promoter activity. Because luciferase expression is regulated both by synthesis and degradation, the process of luciferase expression can be approximated using a consecutive first-order reaction. Therefore, luciferase activity may be more sensitive to stimulation than the promoter activity is, and the increase in sensitivity may depend on the rate of luciferase degradation. Therefore, perhaps a luciferase variant with enhanced sensitivity could be designed by decreasing the degradation rate. At the same time, this phenomenon also means that the luciferase activity may potentially overestimate the promoter activity. To avoid such an overestimation, the rate of luciferase degradation should be increased (compared with that of the signalling pathway) so that the luciferase activity shows a sensitivity similar to that of the promoter activity[36]. However, as the rate of luciferase degradation increases, the amount of luciferase decreases, and the lower detection limit of luciferase decreases. Therefore, a trade-off exists between the lower detection limit of luciferase and the decrease in overestimation. Other probe systems, such as fluorescence resonance energy transfer probes and calcium ion indicators, which have a similar synthesis and degradation framework, share the same problem.

Consecutive first-order reactions can control the sensitivity of downstream molecules to an inhibitor, indicating that the downstream molecule is not always inhibited as strongly as an upstream molecule, even if the target molecule of the inhibitor is inhibited successfully or the downstream network of the target molecule is simple. The sensitivities of the downstream responses to several EGFR inhibitors are reportedly lower than the sensitivities of the upstream molecules[2,3,7,37]. The characteristics of the consecutive first-order reaction may contribute to these decreases in sensitivity, although the decreases in sensitivity may also be caused by other factors, such as the depletion effect in biochemical reactions and the characteristics of network motifs.

Supplementary References

29 Bhalla, U. S., Ram, P. T. & Iyengar, R. MAP kinase phosphatase as a locus of flexibility in a mitogen-activated protein kinase signaling network. *Science* **297**, 1018-1023, (2002).

30 Poritz, M. a., Malmstrom, S., Kim, M. K., Rossmeissl, P. J. & Kamb, A. Graded mode of transcriptional induction in yeast pheromone signalling revealed by single-cell analysis. *Yeast* **18**, 1331-1338, (2001).

31 Shankaran, H., Resat, H. & Wiley, H. S. S. Cell surface receptors for signal transduction and ligand transport - a design principles study. *PLoS Computational Biology* **3**, e101, (2005).

32 Segel, I. H. in *Enzyme Kinetics : Behavior and Analysis of Rapid Equilibrium and Steady-State Enzyme Systems.* 43-44 (Wiley-Interscience, 1993).

33 Barenco, M. *et al.* Ranked prediction of p53 targets using hidden variable dynamic modeling. *Genome biology* **7**, R25, (2006).

34 Tegner, J., Yeung, M. K. S., Hasty, J. & Collins, J. J. Reverse engineering gene networks: integrating genetic perturbations with dynamical modeling. *Proc. Natl. Acad. Sci. U.S.A.* **100**, 5944-5949, (2003).

35 Alon, U. in *An introduction to systems biology: design principles of biological circuits* 5-26 (Chapman & Hall/CRC, 2007).

36 Wang, X., Errede, B. & Elston, T. C. Mathematical analysis and quantification of fluorescent proteins as transcriptional reporters. *Biophys. J.* **94**, 2017-2026, (2008).

37 Cheng, Z.-Y., Li, W.-J., He, F., Zhou, J.-M. & Zhu, X.-F. Synthesis and biological evaluation of 4-aryl-5-cyano-2H-1,2,3-triazoles as inhibitor of HER2 tyrosine kinase. *Bioorganic and Medicinal Chemistry* **15**, 1533-1538, (2007).